Indian J. Phys. **47**, 453-470 (1973)

Laminar flow of a second order fluid between rotating porous disks

SHANKAR PRASAD MISHRA AND GOURANGA CHARAN DASH*

Post-Graduate Department of Mathematics, Utkal University, Bhubaneswar-4, Orissa, India

(*Received* 1 *August* 1972, *revised* 22 *September* 1972)

Steady axially symmetric laminar flow of a second order incompressible fluid between a rotating porous disk and a stationary non-porous disk is considered. The porous disk rotates with a constant angular speed and the suction or injection velocities are assumed to be constant. A perturbation technique has been used to obtain an approximate solution for the velocity field with R, the suction or injection wall Raynolds number as perturbation parameter. Several graphs and tables have been presented to exhibit the effect of the material constants, the rotation coefficient and wall Reynolds number on the velocity components, pressure variation and the skin frictions at the disks.

1 INTRODUCTION

Flow between porous boundaries is of practical as well as of theoretical interest. The practical interest includes problems of gaseous diffusion, boundary cooling, lubrication of porous bearings, etc. Existence of "similar" solutions of the Navier-Stokes equations for some porous boundary problems is also of theoretical interest. Flow through conduits with porous boundaries and uniform suction or injection velocities has been examined by Berman (1956, 1958*a*, 1958*b*), Sellars (1955), Yuan (1956), Yuan & Finkelstein (1956), Elkouh (1967, 1969), Terril (1964) and many others. Mishra (1966), Mishra & Sinha Roy (1967, 1967*a*, 1967*b*, 1968), Bhatnagar (1964) and many others have studied the similar problems with different non-Newtonian liquids. Elkouh (1969) presented a solution for steady axially symmetric laminar flow of an incompressible fluid between a rotating porous disk and a stationary non-porous disk. The porous disk rotates with a constant angular speed, and the suction or injection velocities are assumed constant.

In this paper our aim is to study Elkouh's (1967) problem replacing viscous liquid by a second order liquid. The constitutive equation for a homogeneous,

*Present address : B. J. B. College, Bhubaneswar

isotropic incompressible fluid is developed by Coleman & Noll (1960) and has the form

$$p_{ij} = -p\delta_{ij}+\mu_1 A_{(1)ij}+\mu_2 A_{(2)ij}+\mu_3 A_{(1)ia}A_{(1)aj}, \quad \ldots \quad (1.1)$$

where p_{ij} denotes the stress tensor, p the pressure, μ_1, μ_2, μ_3 are material constants and

$$A_{(1)ij} = v_{i,j}+v_{j,i}; \quad A_{(2)ij} = a_{i,j}+a_{j,i}+2v_{m,i}v_{m,j},$$

v_i being the velocity vector and a_i, the acceleration vector given by

$$a_i = \frac{\partial v_i}{\partial t}+v_k v_{i,k}.$$

2. Formulation of the Problem

We consider a steady laminar flow of a second order liquid between a porous rotating disk and a stationary disk. We use cylindrical polar coordinate system (r, θ, z) We further assume that a constant normal velocity of suction or injection is applied at the disk rotating with a constant velocity In view of this, the velocity field is

$$u_r = u(r, z), \quad u_\theta = v(r, z), \quad u_z = w(r, z). \quad \ldots \quad (2.1)$$

The boundary conditions on the velocity components are

$$\left.\begin{aligned} &u(r, 0) = u(r, h) = w(r, 0) = v(r, 0) = 0, \\ &w(r, h) = -W = \text{constant}, \quad v(r, h) = \Omega_r \end{aligned}\right\} \quad \ldots \quad (2.2)$$

where h is the distance between the disks, W and Ω are, respectively, the constant normal velocity and angular velocity of the disk $z = h$

Following Elkouh (1967) we take

$$\psi(r, \lambda) = \tfrac{1}{2}Wrf(\lambda), \quad \ldots \quad (2.3)$$

where $z = h\lambda$ and ψ is the stream function, such that

$$u = \frac{1}{r}\frac{\partial \psi}{\partial z} = \frac{Wr}{2h}f'(\lambda), \quad w = -\frac{1}{r}\frac{\partial \psi}{\partial r} = -Wf(\lambda) \quad \ldots \quad (2.4)$$

and this is consistent with the equation of continuity. We also assume that

$$v = \Omega_r G(\lambda). \quad \ldots \quad (2.5)$$

Substituting (2.4) and (2.5) stress components are

$$p_{rr} = \frac{\mu_1 W}{h}f'+\frac{\mu_2 W^2}{h^2}\left\{\tfrac{1}{2}f'^2-ff''+\tfrac{1}{2}\frac{r^2}{h^2}f''^2\right\}+\frac{\mu_3 W^2}{h^2}\left\{f'^2+\frac{r^2}{2h^2}f''^2\right\}, \quad \ldots \quad (2.6)$$

$$p_{00} = \frac{\mu_1 W f'}{h} + \frac{\mu_2 W^2}{h^2}\{f'^2 - f''f\} + \frac{\mu_3 W^2}{h^2}\left\{f'^2 + \frac{r^2\Omega^2 G'^2}{W^2}\right\}, \quad \ldots (2.7)$$

$$p_{zz} = -\frac{2\mu_1 W f'}{h} + \frac{2\mu_2 W^2}{h^2}\left(f''f + \frac{r^2}{4h^2}f''^2 + \frac{r^2\Omega^2 G'^2}{W^2} + 2f'^2\right)$$

$$+ \frac{\mu_3 W^2}{h^2}\left(\frac{r^2}{4h^2}f''^2 + \frac{W^2 r^2 G'^2}{W^2} + 4f'^2\right), \quad \ldots (2.8)$$

$$p_{r\theta} = \mu_3 \frac{W\Omega r^2 G' f''}{2h^3}, \quad \ldots (2.9)$$

$$p_{\theta z} = \frac{\Omega\mu_1 r G'}{h} + \frac{\mu_2 W r\Omega}{h^2}(f'G' - fG'') - \frac{\mu_3 W r G' f'\Omega}{h^2} \quad \ldots (2.10)$$

$$p_{zr} = \frac{\mu_1 W r f''}{2h^2} + \frac{\mu_3 W^2 r}{2h^3}(f'f'' - ff''') - \frac{\mu_3 W^2 r}{2h^3} f'f'' \quad \ldots (2.11)$$

The equations of motion, neglecting the azimuthal variations are

$$\rho\left[u\frac{\partial u}{\partial r} + w\frac{\partial u}{\partial z} - \frac{v^2}{r}\right] = -\frac{\partial p}{\partial r} + \frac{\partial p_{rr}}{\partial r} + \frac{\partial p_{rz}}{\partial z} + \frac{p_{rr} - p_{\theta\theta}}{r}, \quad \ldots (2.12)$$

$$\rho\left[u\frac{\partial v}{\partial r} + w\frac{\partial v}{\partial z} + \frac{uv}{r}\right] = \frac{\partial p_{r\theta}}{\partial r} + \frac{\partial p_{\theta z}}{\partial z} + \frac{2}{r}p_{r\theta}, \quad \ldots (2.13)$$

$$\rho\left[u\frac{\partial w}{\partial r} + w\frac{\partial w}{\partial z}\right] = -\frac{\partial p}{\partial z} + \frac{\partial p_{rz}}{\partial r} + \frac{\partial p_{zz}}{\partial z} + \frac{p_{rz}}{r} \quad \ldots (2.14)$$

Substituting the stress components from (2.6)–(2.11) into equations (2.12)–(2.14) we get

$$-\frac{1}{\rho}\frac{\partial p}{\partial r} = \frac{W^2 r}{h^2}\left\{\tfrac{1}{4}f'^2 - \tfrac{1}{2}ff'' - \frac{\Omega^2 h^2}{W^2}G^2\right\} - \frac{\nu_1 W r}{2h^3}f''' - \frac{\nu_2 W^2 r}{2h^4}\{f''^2 - ff^{iv}\} -$$

$$- \frac{\nu_3 W^2 r}{4h^4}\left\{f''^2 - 2f'f''' - \frac{4\Omega^2 h^2 G'^2}{W^2}\right\}, \quad \ldots (2.15)$$

$$f'G - fG' = \frac{\nu_1}{Wh}G'' - \frac{\nu_2}{h^2}(f'''G + f''G' + f'G'' + fG''') + \frac{\nu_3}{h^2}(f''G' - f'G''), \quad \ldots (2.16)$$

$$-\frac{1}{\rho}\frac{\partial p}{\partial\lambda} = W^2 ff' + \frac{\nu_1 W}{h}f'' - \frac{\nu_2 W^2}{h^2}\left\{\tfrac{3}{2}ff''' + 11f'f'' + \frac{r^2}{h^2}f''f'''\right.$$

$$\left. + \frac{2h^2\Omega^2}{W^2}GG'\right\} - \frac{\nu_3 W^2}{h^2}\left\{7f'f'' + \frac{r^2}{2h^2}f''f''' + \frac{3\Omega^2 r^2 G'G''}{W^2}\right\}. \quad \ldots (2.17)$$

Eliminating p between (2.15) and (2.17) and introducing dimensionless parameters

$$R = \frac{Wh}{\nu_1}, \quad S_1 = -\frac{\nu_2}{h^2}, \quad S_2 = \frac{\nu_3}{h^2}, \quad \alpha = \frac{2h^3\Omega^2}{\nu_1 W},$$

we get from (2.15)–(2.17)

$$R(f'G - fG') - G'' = S_1 R(f'''G + f''G' + fG''' + f'G'') + S_2 R(f''G' - f'G''), \quad \ldots (2.18)$$

$$\frac{d}{d\lambda}[f''' + R(ff'' - \tfrac{1}{2}f'^2) + \alpha G^2 R S_1(ff''' + f''^2) - RS_2(\tfrac{1}{2}f''^2 + f'f''') - 4S_2\alpha G'^2] = 0, \quad \ldots (2.19)$$

which on integration gives

$$f''' + R(ff'' - \tfrac{1}{2}f'^2) + \alpha G^2 R S_1(ff'' + f''^2) - RS_2(\tfrac{1}{2}f''^2 + f'f''') - 4S_2\alpha G'^2 = A, \quad \ldots (2.20)$$

where A is a constant of integration. The boundary conditions given in (2.2) in view of (2.4) and (2.5) reduce to

$$f'(0) = f(0) = f'(1) = G(0) = 0, \quad f(1) = G(1) = 1. \quad \ldots (2.21)$$

3. Solution of Equations

To above equations (2.18) and (2.20) we use perturbation technique. R is the perturbation parameter which is assumed to be small. We take

$$\left.\begin{aligned} f(\lambda) &= \sum_{n=0}^{\infty} R^n f_n(\lambda, \alpha), \\ G(\lambda) &= \sum_{n=0}^{\infty} R^n G_n(\lambda, \alpha), \\ A &= \sum_{n=0}^{\infty} R^n A_n(\alpha) \end{aligned}\right\} \quad \ldots (3.1)$$

in which f_n, G_n and A_n are taken to be independent of R. Substituting (3.1) into (2.18) and (2.20) and comparing different powers of R we get zero-th order equations :

$$G_0'' = 0, \quad \ldots (3.2)$$

$$f_0''' + \alpha G_0^2 - 4S_2\alpha G_0'^2 = A_0. \quad \ldots (3.3)$$

First order equations :

$$f'G_0 - f_0G_0' - G_1'' - S_1(f_0'''G_0 + f_0''G_0' + f_0'G_0'' + f_0G_0''') - S_2(G_0'f_0'' - G_0''f_0') = 0, \quad \ldots (3.4)$$

$$f_1''' + f_0f_0'' - \tfrac{1}{2}f_0'^2 + 2\alpha G_0G_1 + S_1(f_0f_0^{iv} + f_0''^2) - \tfrac{1}{2}S_2(f_0''^2 + 2f_0'f_0''') - 8S_2\alpha G_0'G_1' = A_1. \quad \ldots (3.5)$$

Second order equations :

$$f_1'G_0+G_1f_0'-f_0G_1'-f_1G_0'-G_2''-S_1(G_0f_1'''+G_1f_0'''+f_0''G_1'+f_1''G_0'+f_0'G_1''$$
$$+f_1'G_0''+f_1G_0'''+G_1'''f_0)-S_2(G_1'f_0''+f_1''G_0'-G_1''f_0'-f_1'G_0'')=0, \quad \ldots (3\,6)$$

$$f_2'''+f_0f_1''+f_1f_0''-f_0'f_1'+\alpha(G_1^2+2G_0G_2)+S_1(f_1f_0^{iv}+f_1'''f_0+2f_0''f_1'')$$
$$-S_2(f_0''f_1''+f_1'f_0'''+f_0'f_1''')-4\alpha S_2(G_1'^2+2G_0'G_2')=A_2 \quad \ldots (3.7)$$

and so on The boundary conditions to be satisfied by f_n, G_n and their derivatives are

$$\left.\begin{aligned} &f_n(0)=f_n'(0)=f_n'(1)=G_n(0)=0 \text{ for all } n\,; \\ &f_0(1)=G_0(1)=1,\ f_n(1)=G_n(1)=0 \text{ for } n\geqslant 1. \end{aligned}\right\} \quad \ldots (3.8)$$

Solving (3 2) to (3.5) with the boundary conditions given in (3 8) we get, zero-th order solutions as

$$G_0(\lambda)=\lambda \quad \ldots (3.9)$$

$$f_0(\lambda) = (3\lambda^2-2\lambda^3)+\frac{\alpha}{60}(-2\lambda^2+3\lambda^3-\lambda^5) \quad \ldots (3.10)$$

with

$$A_0=\frac{3}{10}\alpha-4\alpha S_2-12.$$

First order solutions as

$$G_1(\lambda)=\frac{1}{20}(-\lambda+5\lambda^4-4\lambda^5)+\frac{\alpha}{12600}\{-8\lambda-35\lambda^4+63\lambda^5-20\lambda^7\}$$
$$-S_1(\lambda+3\lambda^3-4\lambda^3)+S_2(\lambda-3\lambda^2+2\lambda^3)+\frac{\alpha S_1}{30}(\lambda^2-4\lambda^3+2\lambda^5)$$
$$+\frac{\alpha S_2}{60}(2\lambda^2-3\lambda^3+\lambda^5), \quad \ldots (3.11)$$

$$f_1(\lambda)=\frac{1}{70}(13\lambda^2-18\lambda^3+7\lambda^6-2\lambda^7)+\frac{\alpha}{151200}(15\lambda^2+8\lambda^3+252\lambda^5-546\lambda^6$$
$$+216\lambda^7+45\lambda^8+19\lambda^9+\frac{\alpha^2}{9072000}(332\lambda^2-579\lambda^3+192\lambda^5+252\lambda^6$$
$$-162\lambda^7-30\lambda^8-15\lambda^9+10\lambda^{11})+\frac{1}{10}S_1(3\lambda^2+14\lambda^3-45\lambda^4+36\lambda^5-8\lambda^6)$$
$$+\frac{1}{20}S_2(-15\lambda^2+34\lambda^3-15\lambda^4-12\lambda^5+8\lambda^6)+\frac{1}{4200}\alpha S_1(662\lambda^2$$

$$-1094\lambda^3+595\lambda^4-476\lambda^5+168\lambda^6+210\lambda^7-65\lambda^8)+\frac{\alpha S_2}{58800}(2170\lambda^2$$

$$-4718\lambda^3+2205\lambda^4-1176\lambda^5+4214\lambda^6-3150\lambda^7+455\lambda^8)+\frac{S_1\alpha^2}{4536000}$$

$$\times(16031\lambda^2-20350\lambda^3-4620\lambda^4+6426\lambda^5+2268\lambda^6-780\lambda^7+1755\lambda^8$$

$$-450\lambda^9-280\lambda^{10})+\frac{S_2\alpha^2}{117936000}(-120419\lambda^2+179894\lambda^3-38220\lambda^4$$

$$+4914\lambda^5-62244\lambda^6+74100\lambda^7-22815\lambda^8-18850\lambda^9+3640\lambda^{10})$$

$$+\tfrac{2}{9}S_1S_2\alpha(3\lambda^2-2\lambda^3-5\lambda^4+4\lambda^5)+\frac{S_1S_2\alpha^2}{1575}(-11\lambda^2+19\lambda^3+35\lambda^4$$

$$-63\lambda^5+20\lambda^7)+\tfrac{2}{5}\alpha S_2^2(-\lambda^2+4\lambda^3-5\lambda^4+2\lambda^5)+\frac{1}{3150}\alpha^2S_2^2$$

$$(-16\lambda^2-\lambda^3+70\lambda^4-63\lambda^5+10\lambda^7), \qquad \ldots (3.12)$$

with

$$A_1=-\frac{54}{35}+\frac{\alpha}{3150}-\frac{193\alpha^2}{504000}+\frac{42}{5}S_1+\frac{51}{5}S_2-\frac{547}{350}\alpha S_1-\frac{407}{15120}\alpha^2S_1$$

$$-\frac{171}{2100}\alpha S_2+\frac{10759}{756000}\alpha^2S_2+\frac{16}{5}S_1S_2\alpha+\frac{38}{525}S_1S_2\alpha^2+\tfrac{8}{5}S_2^2\alpha-\frac{S_2^2\alpha^2}{525}.$$

It has been shown by Elkouh (1969) that the first order perturbation solution is sufficiently accurate for $R<1$. We also see that this conclusion is true for a second order fluid The expression for A_2 is

$$A_2=-0{\cdot}064007+0{\cdot}005293\alpha+0{\cdot}000051\alpha^2+0{\cdot}0000006\alpha^3-0{\cdot}325S_1$$

$$-0{\cdot}611S_2-0{\cdot}2167\alpha S_1-0{\cdot}0043\alpha S_2-0{\cdot}00086\alpha^2S_1+0{\cdot}00021\alpha^2S_2$$

$$-0{\cdot}000011S_1^2-0{\cdot}000031S_2^2-0{\cdot}000001S_1S_2-0{\cdot}00352\alpha S_1^2$$

$$-0{\cdot}000016\alpha S_2^2+0{\cdot}0000001\alpha S_1S_2+0{\cdot}0000001\alpha^2S_1^2+$$

$$+0{\cdot}0000002\alpha^2S_2^2-0{\cdot}00000001\alpha^2S_1S_2-0{\cdot}00000002\alpha^3S_1^2$$

$$+0{\cdot}00000001\alpha^3S_2^2-0{\cdot}000000001\alpha^3S_1S_2 \qquad \ldots (31.13)$$

Tables 1 and 2 show that the values of A_2 are very small and increase in the value of S_1 and S_2 decreases it further So a first order solution is considered sufficiently accurate for $R\leqslant 1$. So we can take

Table 1 Values of A_2 for various values of α and S_1 when $S_2 = 0$

S_1 \ α	0	10	20	30
0.00	−0 064007	−0.005372	0.066923	0.156335
0 01	−0.067257	−0.021157	0.01707	0.08088

Table 2 Values of A_2 for various values of α and S_2 when $S_1 = 0$ 0·01.

S_2 \ α	0	10	20	30
0 00	−0.067257	−0.021157	0.01707	0.08088
0.01	−0.073367	−0.037487	0.01039	0.04123

$$\left.\begin{aligned} G(\lambda) &= G_0(\lambda)+RG_1(\lambda)+0(R^2). \\ f(\lambda) &= f_0(\lambda)+Rf_1(\lambda)+0(R^2), \\ A &= A_0+A_1R+0(R^2), \end{aligned}\right\} \quad \ldots (3.15)$$

with

where the velocity distribution in the radial, in the z-direction and in the tangential direction are, respectively .

$$\frac{u}{[u]} = f' = f_0'+Rf_1', \quad \ldots (3.15)$$

where $[u]$ = the average velocity in the radial direction, that is,

$$[u] = \int_0^1 u \, d\lambda = \frac{Wr}{2h}, \quad \ldots (3.16)$$

$$\frac{w}{W} = -f(\lambda) = -(f_0+Rf_1), \quad \ldots (3.17)$$

and

$$\frac{v}{\Omega r} = G(\lambda) = G_0+RG_1. \quad \ldots (3.18)$$

With the help of (2.15) and (2.17) the dimensionless pressure coefficient p^* is

$$p^* = \frac{p(r,\lambda)-p(a,\lambda)}{\frac{1}{2}\rho W^2} \left(\frac{h}{a}\right)^2,$$

$$= \frac{1}{2R}\left[[A-2S_1Rf''^2+RS_2f''^2+3\alpha S_2G'^2] \left(\frac{r^2}{a^2}-1\right) \right]. \quad \ldots (3.19)$$

Equation (3.19) is valid for injection flows. For suction flows substituting for R and α the negative values in (3.19) we get the pressure distribution.

The shear stress $p_{\theta z}$ on the rotating disk is given by

$$p_{0z}]_{z=h} = \frac{\Omega\mu_1 r}{h}[G'(\lambda) - RS_1\{f'(\lambda)G'(\lambda) - f(\lambda)G''(\lambda)\} - RS_2 f'(\lambda)G'(\lambda)]_{\lambda=1}$$

$$= \frac{\Omega\mu_1 r}{h}\left[1 - \frac{R}{20} + \frac{3R\alpha}{1400} + 5RS_1 + RS_2 + \frac{1}{10}R\alpha S\right]. \quad \ldots (3.20)$$

Multiplying (3.20) by $2\pi r^2\,dr$ and integrating between the limits $r = 0$ and $r = a$, the following expression for the resisting moment

$$M = \int_0^a p_{\theta z}\,2\pi r^2\,dr = \frac{\pi\mu_1\Omega a^4}{2h}\left[1 - \frac{R}{20} + \frac{3\alpha R}{1400} + 5RS_1 + RS_2 + \frac{1}{10}R\alpha S_1\right]$$

is obtained. The dimensionless moment coefficient is

$$C_M = \frac{M}{\frac{1}{2}\pi\rho\Omega^2 a^5} = \frac{1}{R_M}\left(\frac{a}{h}\right)\left[1 - \frac{R}{20} + \frac{3\alpha R}{1400} + 5RS_1 + RS_2 + \frac{R\alpha S_1}{10}\right], \quad \ldots (3.21)$$

where $R_M = \Omega a^2/\nu_1$ is a Reynolds number based on the radius of the disk and the tip velocity.

The shear stress p_{rz} at the either disk is given by

$$p_{rz} \quad \frac{\mu_1 |u|}{h}[f''(\lambda) - RS_1\{f'(\lambda)f''(\lambda) - f(\lambda)f'''(\lambda)\} - RS_2 f'(\lambda)f''(\lambda)]. \quad \ldots (3.22)$$

Conclusions

Solution has been obtained for $R < 1$. But in the numerical calculations we have taken $R = 1$. As it is seen that even when $|R| = 1$, the various order corrections decrease very rapidly.

Velocity field. In the absence of suction or injection and rotation coefficient we get from (2.15)

$$\frac{u}{|u|} = 6\lambda(1-\lambda)$$

which is the usual Poiseuille flow between two impermeable walls.

(*i*) *Radial velocity distribution.* Figure 1 shows that the velocity curves for different values of R intersect each other at a point. This also shows that the effect of cross-viscosity is to shift the point of intersection towards the rotating disk. From the stationary disk up to this point of intersection, the velocity at any point increases with the increase in the value of R and S_2 increases it

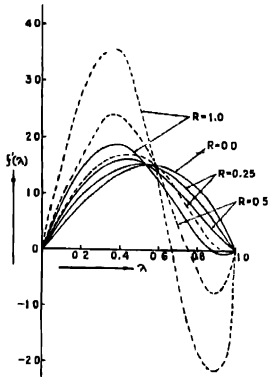

Figure 1. Radial velocity distribution for different values and S_2 when $\alpha = 20$, $S_1 = 0{\cdot}5$, $S_2 = 0{\cdot}5$ – – – –, $S_3 = 0.0$ ————

further But in the liquid layer near the rotating disk an opposite effect is observed. In this layer only for higher values of R, inflexion point appears in the curve But with cross-viscosity even for smaller values of R an inflexion point appears. Figure 2 shows that velocity in the liquid layer from the stationary disk up to the point of intersection of the velocity curves for different values of α decreases as α increases, but the elasticity of the liquid increases the velocity at that point Beyond this layer an opposite effect is observed. This figure also suggests that for higher values of α, an inflexion point might appear near

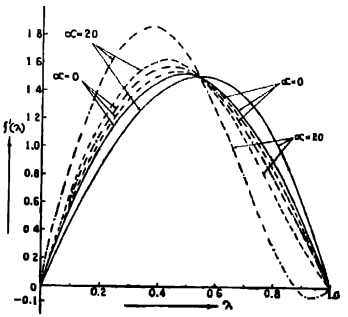

Figure 2. Radial velocity distribution for different values of S_1 and α, when $S_2 = 0$ and $R = 1$, $S_3 = 0{\cdot}25$ – – – – –, $S_3 = 0{\cdot}5$–.–.–.–.–.–.–, $S_3 = 0{\cdot}0$ ————

the rotating disk. Also, for $R = 1$, an inflexion point at the stationary disk occurs for the values of α given by the equation

$$(-13{\cdot}54286+8{\cdot}4S_1+10{\cdot}4S_2)+\alpha(0{\cdot}30032-1{\cdot}562858S_1-0{\cdot}48143S_2 -4{\cdot}8S_1S_2+9{\cdot}6S_2^2)+\alpha^2(-0{\cdot}00038-0{\cdot}02692S_1+0{\cdot}00915S_2 +0{\cdot}07238S_1S_2-0{\cdot}0019S_2^2) = 0.$$

Table 3 gives the values of α for different values of S_1 and S_2. When $S_1 = S_2 = 0$, out of two values of α, namely 48·0115 and 742·3043 Elkouh (1967) has retained the value 48·0115, but non-zero values of S_1 and S_2 indicate that the other value 742·3043 should be accepted, so that for a fixed value of S_2 an increase in the

Table 3. Values of α for the appearence of an inflexion point at the stationary disk when $R = 1$

S_2 \ S_1	0 00	0 01	0 02
0 00	48 0114 (Elkouh's case) 742.3043	53.5360	66.4743
0 01	979.4040	94 6808	66.8014
0.02	1442 5949	95.8379	67 2001

value of S_1 will put α in a regular order, that is, will decrease the value of α So elasticity of the liquid decreases the value of α for the appearance of an inflexion point But the cross-viscosity increases the value of α for the appearance of an inflexion point. When the disk rotates in opposite sense, figure 3 shows that the elasticity of the liquid decreases the velocity for $0 < \lambda < 0{\cdot}54$ and then an opposite effect is observed. Figure 4 shows that the velocity at any point increases with S_2 when $0 < \lambda < 0{\cdot}52$ and an opposite effect is observed when $0{\cdot}52 < \lambda < 1$. When $S_2 = 0$ the velocity is positive between the disks

(*ii*) *Tangential velocity distribution*. Figure 5 shows that the velocity at any point decreases as R increases. The cross-viscosity affects the velocity for non-zero values of R. S_2 increases the velocity when $0 < \lambda < 0{\cdot}6$ (nearly) and beyond this an opposite effect is observed. Figure 6 shows that the velocity curves for different values of α intersect at the point $\lambda = 0{\cdot}465$ (nearly) The velocity at any point in $0 < \lambda < 0{\cdot}465$ increases with the increase in the value of α, and an opposite effect is observed beyond this layer This figure also shows that a point of inflexion appears at the point of intersection. Figure 7 shows that the velocity is almost a straight line for $S_1 = 0$ but with the increase in the value of S_1 the velocity decreases at any point For higher values of S_1 inflexion point appears on the curves for velocity field. Figure 8 shows the velocity curves

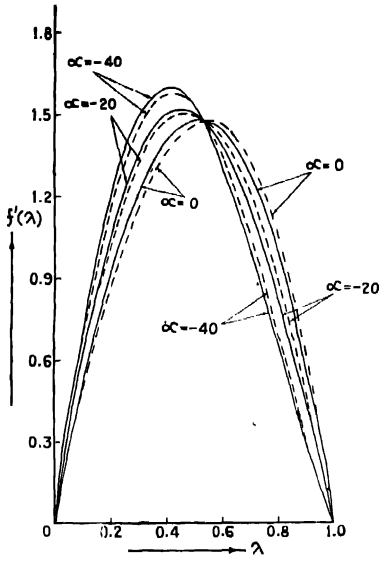

Figure 3. **Radial velocity distribution for different values of α and S_1 when $R = -1$ and $S_2 = 0$, $S_1 = 0{\cdot}0$ ————, $S_2 = 0{\cdot}25$ - - - - -**

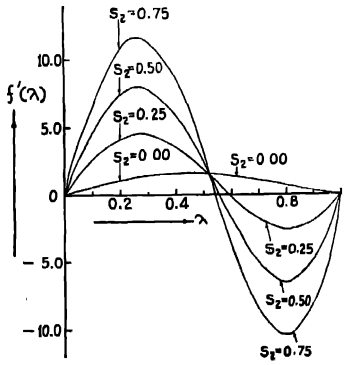

Figure 4. **Radial velocity distribution for different values of S_2, $\alpha = -40$, $R = -1$, and $S_1 = 0{\cdot}75$.**

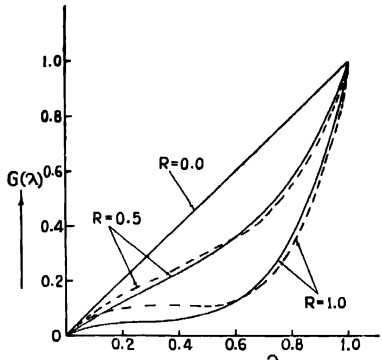

Figure 5. Transversal velocity distribution for different values of R and S_2 when $S_1 = 0.5$ and $\alpha = 20$, $S_2 = 0$ ————, $S_2 = 0.5$ – – – –

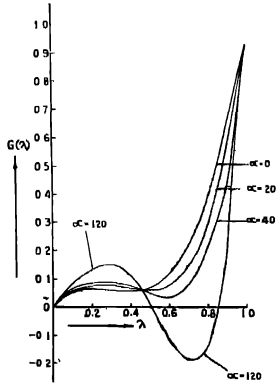

Figure 6. Transversal velocity distribution for different values of α, $S_1 = 0.75$, $R = 0.75$, $S_2 = 0.5$

for different values of S_2 intersect at the point $\lambda = 0.36$ for negative values of R and α The velocity at any point decreases as S_2 increases for $0. < \lambda < 0.36$ But an opposite effect of pronounced nature is observed for $0.36 < \lambda < 1$.

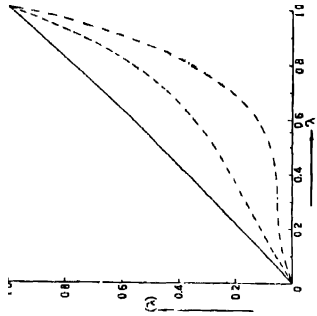

Figure 7. Transversal velocity distribution for different values of S_1, $R = 1$, $\alpha = 20$, $S_2 = 0\cdot0$, $S_1 = 0\cdot00$ ————, $S_2 = 0\cdot25$ – – – –, $S_1 = 0\cdot5$ –.–.–.–.–

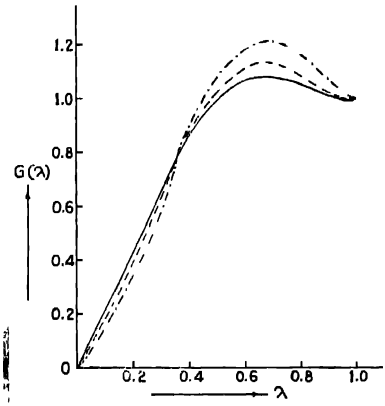

Figure 8. Transversal velocity distribution for different values of S_2, $R = -1$, $\alpha = -40$, $S_1 = 0\cdot75$, $S_2 = 0$ ————, $S_2 = 0\cdot25$ – – – – –, $S_2 = 0\cdot75$ –.–.–.–.–.–

(*iii*) *Axial velocity components* : Figures 9, 10, 11, 12 show that—

(a) When S_1 and α are fixed, velocity component decreases as R increases and the effect of S_2 is to decrease the velocity at any point for both sense of rotation.

(b) When R, α and S_2 are fixed, velocity at any point decreases as S_1 increases.

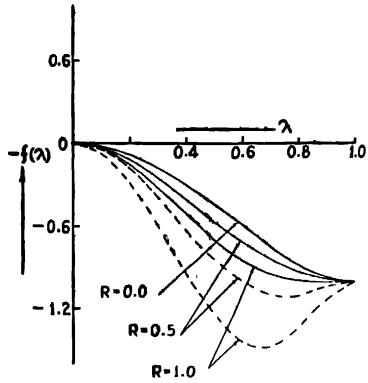

Figure 9. Axial velocity distribution for different values of R and different values of S_2 when $S_1 = 0{\cdot}5$, $\alpha = 20$, $S_2 = 0\,0$ ————, $S_2 = 0{\cdot}5$ - - - - -

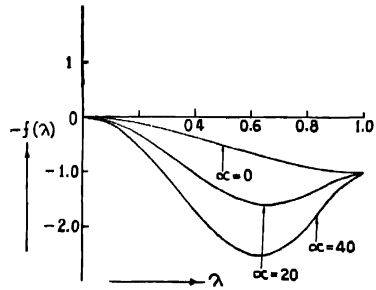

Figure 10. Axial velocity distribution for different values of α, when $S_1 = 0{\cdot}75$, $R = 0\,75$ and $S_2 = 0{\cdot}5$.

(c) When R, S_1 and S_2 are fixed, velocity at any point decreases as α increases.

Pressure distribution. Figure 13 shows that P decreases as the values of R increases But for a certain value of R, the elasticity of the liquid increases P in the middle of the channel. Figure 14 represents the pressure disbtribution at $\lambda = 0{\cdot}5$. Being negative, as α increases, the pressure decreases and the elastic elements decrease P further.

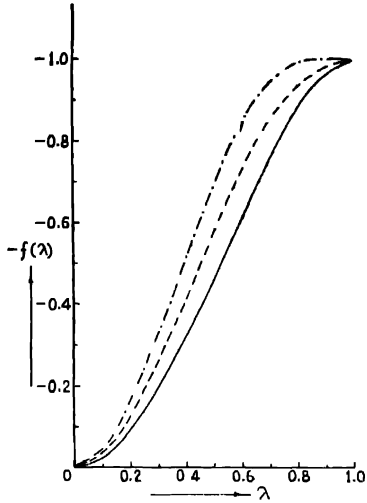

Figure 11 Axial velocity distribution for different values of S_1 when $R = 1$, $\alpha = 20$, $S_2 = 0$, $S_1 = 0{\cdot}00$ ————, $S_1 = 0{\cdot}25$ - - - -, $S_2 = 0{\cdot}5$ -.-.-.-.-

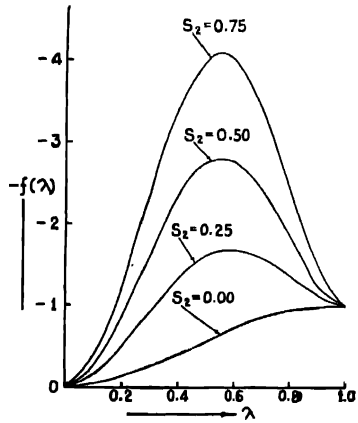

Figure 12. Axial velocity distribution for different values of S_2 when $R = -1$, $\alpha = -40$ $S_1 = 0{\cdot}75$

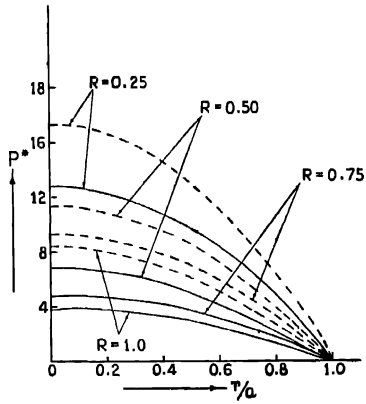

Figure 13. Pressure distribution for different values of R and S_1 when $S_2 = 0.0$ and $\alpha = 20$, $\lambda = 0.5$, $S_1 = 0.0$ ————, $S_1 = 0.25$ – – – –

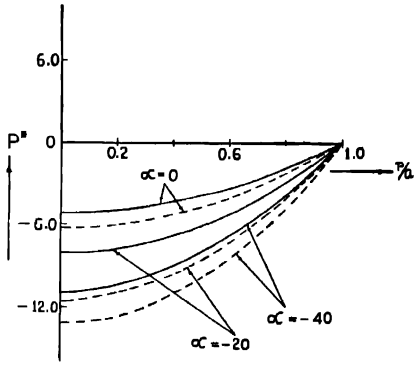

Figure 14 Pressure distribution for different values of α and S_1 at the middle of the channel $R = -1$, $S_2 = 0.0$, $S_1 = 0$ ————, $S_1 = 0.25$ – – – –

Moment coefficient · Moment coefficient increases with the increase of R, α and S_1 at the rotating disk but an opposite effect is observed at the stationary disk (tables 4, 5, 6). When $R = 0$, it is equal to one for both the disks. S_2 decreases the moment coefficient at both the disks for suction flow (table 7).

Table 4 Moment coefficient for different values of R. $S_1 = 0{\cdot}5$, $S_2 = 0{\cdot}5$, $\alpha = 20$

disk \ R	0	0.25	0.5	0 75	1.0
Lower	1	0.9987	0 9976	0 9956	0.9134
Upper	1	2.0001	3 0002	4.0005	5 0006

Table 5. Moment coefficient for different values of α. $S_1 = 0{\cdot}75$, $S_2 = 0{\cdot}5$, $R = 0{\cdot}75$

disk \ α	0	10	20	30	40
Upper	4 1235	4.4732	5 2537	5 6532	6 4032
Lower	0 8035	0 7935	0 7535	0.7225	0 7035

Table 6 Moment coefficient for different values of S_1. $S_2 = 0{\cdot}5$, $\alpha = 40$, $R = 0{\cdot}5$.

disk \ S_1	0	0 25	0 5	0.75
Upper	1.2503	2.3505	3 5504	4.6321
Lower	1.2053	1 0537	0 9537	0 8325

Table 7 Moment coefficient for different values of S_2 $R = -1$, $\alpha = -40$, $S_1 = 0{\cdot}75$

disk \ S_2	0	0.25	0 5	0 75
Upper	0 3506	0 1503	−0 1034	−0 3537
Lower	1.7034	1 4506	1 2506	1 0027

Radial shearing stress · The radial shearing stress p_{rz} is given by

$$\tau_i = \frac{hp_{rz}}{\mu_1[u]} = f''(\lambda) - RS_1\{f'(\lambda)f''(\lambda) - f(\lambda)f'''(\lambda)\} - RS_2 f'(\lambda)f''(\lambda),$$

where τ $(i = 0, 1)$ for $\lambda = 0$ and 1 represents radial shearing stress at the lower and upper disk, respectively.

When $\tau_0 = 0$, an increase in R and S_1 results in an increase in the value of α (table 8). Table shows that the value of α decreases as S_2 increases For the injection, flow reversal occurs near the stationary disk for values $\alpha < 90$. For $R = 1$, incipient flow reversal is at $\alpha = 108{\cdot}9206$ and elasticity increases it, while

the cross viscosity decreases it. Table 10 shows that at both the disks the shearing stress increases as R increases. But the shearing stress at the rotating disks increases rapidly.

R \ S_1	0	0.01	0.02
0.0	90.000	90.000	90 000
0 5	98.2286	108.1767	123 3973
1.0	108.9206	156.0820	240.6745

Table 9. Values of α for $\tau_0 = 0$ when $S_1 = 0$

R \ S_2	0	0.01	0.02
0.00	90.00	90.00	90.00
0.5	98 2286	96 9441	95.4641
1.0	108.9206	105.3088	101.5617

Table 10. Radial shearing stress for different values of R $\alpha = 20$, $S_1 = S_2 = 0{\cdot}5$

Disk \ R	0	0 25	0 5	0.75	1
Upper	−8 1257	0 1927	8.5231	16 5724	25.9225
Lowor	4.5246	6.5243	9.5125	11 8732	14.5239

References

Borman A. S. 1956 *J Appl. Phys* **27**, 1557.

1958a *Proc. 2nd Intern. Congr Pearcful Uuses of Atomic Energy*, Geneva, **4**, 351.

1958b *J. Appl. Phys.* 29, **29.**

Bhatnagar R. K. 1963 *J. Ind. Inst. Sci.* **45(4)**, 126.

Colaman B. D. & Noll W 1960 *Arch Rato. Mech. Anal.* **6**, 353.

Elkouh A. F. 1967 *J. Engg. Mech. Div. ASCE*, 93, No. EMA, 31.

Elkouh A. F. 1969 *Appl. Sci. Res.* **21**, 284.

Mishra S. P. 1966 *J Appl Phys.* **37**, 198

Mishra S. P & Sinha Roy, J. 1967 *Proc. Summer Seminar in Fluid Dynamics held at I.I.Sc., Bangalore*, May 1967, 330.

1967a *J. Appl. Phys.* **38**, 2072.

1967b *The Phys. Fluids* **10**, 2300.

1968 *Appl. Phys. Quart* **10**, 10.

Sellars J R. 1955 *J. Appl Phys.* **29**. 489.

Torril R M. 1964 *Aero. Quart* **15**, 299.

Yuan S W. & Finkelstein A. B. 1956 *Trans. ASME.* **78**, 719.

Yuan S. W. 1956 *J. Appl. Phys.* **27**, 267.